Paper AAS 03-630

American Astronautical Society

American Institute of Aeronautics and Astronautics

Simple Control Laws for Low-Thrust Orbit Transfers

Anastassios E. Petropoulos
Senior Member of the Engineering Staff
Jet Propulsion Laboratory,
California Institute of Technology,
Pasadena, CA 91109-8099, USA.

AAS/AIAA Astrodynamics Specialists Conference

Big Sky Resort, Big Sky, Montana August 3–7, 2003
AAS Publications Office, P.O. Box 28130, San Diego, CA 92198

AAS 03-630

SIMPLE CONTROL LAWS FOR LOW-THRUST ORBIT TRANSFERS

Anastassios E. Petropoulos*

Two methods are presented by which to determine both a thrust direction and when to apply thrust to effect specified changes in any of the orbit elements except for true anomaly, which is assumed free. The central body is assumed to be a point mass, and the initial and final orbits are assumed closed. Thrust, when on, is of a constant value, and specific impulse is constant. The thrust profiles derived from the two methods are not propellant-optimal, but are based firstly on the optimal thrust directions and location on the osculating orbit for changing each of the orbit elements and secondly on the desired changes in the orbit elements. Two examples of transfers are presented, one in semimajor axis and inclination, and one in semimajor axis and eccentricity. The latter compares favourably with a propellant-optimized transfer between the same orbits. The control laws have few input parameters, but can still capture the complexity of a wide variety of orbit transfers.

INTRODUCTION

With the aim of providing both simple approximations to, and good initial guesses for, propellant-optimal, low-thrust orbit transfers which involve specified changes in all orbit elements except true anomaly, we develop control laws which have but few input parameters yet capture the complexity of a wide variety of orbit transfers. As approximations, the control laws provide mission designers with rapid estimates of propellant requirements and times of flight, as well as the trade-offs between the two. In providing initial guesses for optimisation, the control law would be particularly useful for the case where large numbers of revolutions are required. Both continuous and intermittent thrusting are permitted for the transfer, but no constraints are placed on when thrusting can occur. When non-zero, the thrust is assumed to be constant, and the specific impulse is similarly constant. The central body is modelled as a point mass, and the initial and final orbits are assumed closed. No perturbing forces are considered.

The control laws build on the ideas of Kluever[1], and Gefert and Hack[2], who "blend" the instantaneously optimal thrust directions for changing each of the orbit elements. In this paper we develop two concepts for obtaining control laws, and provide examples of such control laws. The concepts are both based on knowledge not only of the optimal thrust direction for changing each of the orbit elements, but also on knowledge of the optimal location on the osculating orbit for effecting such a change, and the corresponding maximum rate of change for each orbit element. The first concept may be termed a "time-to-go" concept, as it is based on conservative lower bounds on the times needed to effect the desired changes in each of the orbit elements. The second concept relies on what may be termed a "proximity quotient," that is, an assessment of the proximity to the final orbit, and its time rate of change.

The first of the following sections presents analytic expressions for the maximum rates of change

*Senior Member of the Engineering Staff, Jet Propulsion Laboratory, California Institute of Technology, Pasadena, CA 91109-8099, USA. Member AAS. Member AIAA. Email: Anastassios.Petropoulos@jpl.nasa.govCopyright © 2003 by Anastassios E. Petropoulos. Published by the American Astronautical Society with permission.

for each of the orbit elements, the optimal thrust directions, and the optimal orbital locations for effecting change in the orbit element. In the case of argument of periapsis, in-plane thrust is assumed. The second and third sections describe the time-to-go concept and the proximity quotient concept, respectively, along with numerical examples. In the fourth section, one of the numerical examples is compared with a propellant-optimal transfer between the same orbits.

ANALYSIS

We commence with Gauss's form of the variational equations for the orbit:[3]

$$\frac{\mathrm{d}\Omega}{\mathrm{d}t} = \frac{r\sin(\theta+\omega)}{h\sin i} f_h \tag{1}$$

$$\frac{\mathrm{d}i}{\mathrm{d}t} = \frac{r\cos(\theta+\omega)}{h} f_h \tag{2}$$

$$\frac{\mathrm{d}\omega}{\mathrm{d}t} = \frac{1}{eh}\left[-p\cos\theta f_r + (p+r)\sin\theta f_\theta\right] - \frac{r\sin(\theta+\omega)\cos i}{h\sin i} f_h \tag{3}$$

$$\frac{\mathrm{d}a}{\mathrm{d}t} = \frac{2a^2}{h}\left(e\sin\theta f_r + \frac{p}{r} f_\theta\right) \tag{4}$$

$$\frac{\mathrm{d}e}{\mathrm{d}t} = \frac{1}{h}\left\{p\sin\theta f_r + \left[(p+r)\cos\theta + re\right] f_\theta\right\} \tag{5}$$

$$\frac{\mathrm{d}\theta}{\mathrm{d}t} = \frac{h}{r^2} + \frac{1}{eh}\left[p\cos\theta f_r - (p+r)\sin\theta f_\theta\right] \tag{6}$$

The nomenclature for these and subsequent equations is explained in the Notation section. The components f_r, f_θ, and f_h of the thrust acceleration are given in terms of the thrust acceleration and the thrust angles as:

$$\begin{aligned} f_r &= f\cos\beta\sin\alpha \\ f_\theta &= f\cos\beta\cos\alpha \\ f_r &= f\sin\beta \end{aligned}$$

It is often of interest to attain prescribed changes in the elements except for true anomaly. That is, the position of departure from the initial and the position of arrival onto the final orbit are often immaterial. With this in mind, we concern ourselves only with the first five variational equations. For each orbit element, we derive the thrust direction which maximises the rate of change of that orbit element at any given position on the orbit, the position (or positions) on the orbit where that maximum rate is at its maximum, and the value of the corresponding rate of change in the orbit element. As we shall note in a later subsection, the thrust direction and the rate of change for maximally increasing an orbit element are simply related to those for maximally decreasing the orbit element, so for simplicity we will develop only the maximal increase case in detail.

For a particular orbit element, the thrust direction maximising its rate of change is found by simply setting to zero the partial derivative of the right hand side of the variational equation for that element with respect to the thrust angle. To find the location on the orbit where the rate of change is maximised, the partial derivative is taken instead with respect to the true anomaly. This procedure is described more explicitly in the subsection for the argument of periapsis.

Semimajor Axis

It is well known that thrust along the velocity vector maximises the rate of increase of semimajor axis, while thrust against the velocity maximises the rate of decrease of semimajor axis. The

two rates are equal. The greatest maximum rate of change can be achieved at periapsis. These observations arise immediately from Eq. (4) and various well-known relations for conic orbits. Specifically, we may write for the maximum rates of change and the related thrust angle:

$$\alpha_{\mathrm{x}} = \gamma \tag{7}$$

$$\alpha_{\mathrm{xx}} = 0 \tag{8}$$

$$\dot{a}_{\mathrm{x}} = \frac{2a^2 v}{\mu} f \sin(\alpha - \gamma) \tag{9}$$

$$\dot{a}_{\mathrm{xx}} = 2f\sqrt{\frac{a^3(1+e)}{\mu(1-e)}} \tag{10}$$

$$\theta_{\mathrm{xx}} = 0 \tag{11}$$

Of course, the out-of-plane thrust is zero.

Eccentricity

Various authors have derived the optimum thrust angle for changing eccentricity:[2]

$$R\sin\alpha_{\mathrm{x}} = e(1+e\cos\theta)\sin\theta \tag{12}$$

$$R\cos\alpha_{\mathrm{x}} = (1+e\cos\theta)^2 - (1-e^2) \tag{13}$$

or, equivalently

$$R\sin\alpha_{\mathrm{x}} = \sin\theta$$

$$R\cos\alpha_{\mathrm{x}} = \cos E + \cos\theta$$

We add here a derivation of where on the orbit a local maximum is achieved in $\dot{e}$. From Eq. (5) we may easily obtain the partial derivative

$$\frac{\partial\dot{e}}{\partial\theta} = \frac{1}{h}\left\{p\cos\theta f_r + \left[-(p+r)\sin\theta + \frac{\partial r}{\partial\theta}\cos\theta + e\frac{\partial r}{\partial\theta}\right] f_\theta\right\} \tag{14}$$

By simple inspection of Eqs. (5), (12), (13), and (14), we see that $\theta = \pi$ yields a local maximum of $\dot{e}_{\mathrm{x}}$ over θ. It is difficult to determine analytically whether other maxima exist, but physical insight and a small numerical study suggest that the local maximum at apoapsis is the only one, and hence the global maximum. Thus we may write

$$\dot{e}_{\mathrm{xx}} = \frac{2pf}{h} \tag{15}$$

$$\theta_{\mathrm{xx}} = \pi \tag{16}$$

Argument of Periapsis

Due to the complexity of the right hand side of Eq. (3), we shall derive here only the optimum in-plane thrust angle and associated optimum orbit location for changing the argument of periapsis. That is, we assume that $f_h = 0$, meaning that the orbit plane remains unchanged. Equation (3) may thus be written

$$\frac{\mathrm{d}\omega}{\mathrm{d}t} = \frac{1}{eh}\left[-p\cos\theta f_r + (p+r)\sin\theta f_\theta\right] \tag{17}$$

The thrust angle giving the maximum rate of change of ω is found by solving for α the equation

$$\frac{\partial\dot{\omega}}{\partial\alpha} = 0 \tag{18}$$

and checking whether the resulting values of α give maximum or minimum $\dot{\omega}$ in Eq. (17). After a brief derivation, we find

$$R\sin\alpha_{\mathrm{x}} = -p\cos\theta \tag{19}$$

$$R\cos\alpha_{\mathrm{x}} = (p+r)\sin\theta \tag{20}$$

Similar expressions for α_{x} are given by Gefert and Hack.[2] The angle α_{x} gives the maximum $\dot{\omega}$,

$$\dot{\omega}_{\mathrm{x}} = \frac{f}{eh}\sqrt{p^2\cos^2\theta + (p+r)^2\sin^2\theta} \tag{21}$$

It is easy to show that the minimum $\dot{\omega}$ is given as $\dot{\omega}_{\mathrm{n}} = -\omega_{\mathrm{x}}$, with the corresponding thrust angle $\alpha_{\mathrm{n}} = \alpha_{\mathrm{x}} + \pi$.

To find the true anomaly where $\dot{\omega}_{\mathrm{x}}$ reaches its maximum value, $\dot{\omega}_{\mathrm{xx}}$, we first rewrite Eq. (17) in a more convenient form:

$$\dot{\omega} = \frac{fA}{eh}\sin(\theta - \phi) \tag{22}$$

where

$$A = \sqrt{p^2\sin^2\alpha + (p+r)^2\cos^2\alpha} \tag{23}$$

$$\tan\phi = \frac{p}{p+r}\tan\alpha \tag{24}$$

The partial derivative of $\dot{\omega}$ with respect to θ is then obtained as

$$\frac{\partial\dot{\omega}}{\partial\theta} = \frac{f}{eh}\left[\frac{\partial A}{\partial r}\frac{\partial r}{\partial\theta}\sin(\theta-\phi) + A\cos(\theta-\phi)\frac{\partial(\theta-\phi)}{\partial\theta}\right] \tag{25}$$

Setting the right-hand side of Eq. (25) equal to zero will satisfy the necessary condition for the true anomaly where $\dot{\omega}$ is greatest. This necessary condition, together with the optimal thrust angle of Eqs. (19) and (20), and the knowledge that $\dot{\omega}_{\mathrm{n}} = -\omega_{\mathrm{x}}$, may be solved, after various manipulations, to yield the cubic equation

$$e^2\cos^3\theta_{\mathrm{xx}} + 3e\cos^2\theta_{\mathrm{xx}} + (3+e^2)\cos\theta_{\mathrm{xx}} + 2e = 0 \tag{26}$$

Analytic solutions being available for cubic equations, we find that there is one real root for $\cos\theta_{\mathrm{xx}}$, which is given by

$$\cos\theta_{\mathrm{xx}} = \left[\frac{1-e^2}{e^3} + \sqrt{\frac{1}{4}\left(\frac{1-e^2}{e^3}\right)^2 + \frac{1}{27}}\right]^{\frac{1}{3}} - \left[-\frac{1-e^2}{e^3} + \sqrt{\frac{1}{4}\left(\frac{1-e^2}{e^3}\right)^2 + \frac{1}{27}}\right]^{\frac{1}{3}} - \frac{1}{e} \tag{27}$$

Equation (27) thus provides the true anomaly where $\dot{\omega}_{\mathrm{x}}$ is at its maximum, that is, where ω can best be changed. The value of $\dot{\omega}_{\mathrm{xx}}$ is obtained by substituting for θ in Eq. (21) from Eq. 27):

$$\dot{\omega}_{\mathrm{xx}} = \dot{\omega}_{\mathrm{x}}(\theta = \theta_{\mathrm{xx}}) \tag{28}$$

It may be possible, if more involved, to include in a similar vein the effect of the out-of-plane thrust on the argument of periapsis.

Inclination

Clearly from Eq. (2), the optimum thrust angle for increasing the inclination is

$$\beta_{\mathrm{x}} = \mathrm{sgn}[\cos(\theta+\omega)]\frac{\pi}{2} \tag{29}$$

which gives the maximum $\dot{i}$ as

$$\dot{i}_{\mathrm{x}} = \frac{r|\cos(\theta+\omega)|}{h} f \tag{30}$$

By setting $\partial\dot{i}/\partial\theta = 0$, we find the necessary condition for the optimum true anomaly at which to change i:

$$\sin(\theta_{\mathrm{x}} + \omega) = -e\sin\omega \tag{31}$$

The quadrant uncertainty for θ in Eq. (31) is resolved by noting that the quadrant giving the maximum r yields the maximum $\dot{i}_{\mathrm{x}}$ in Eq. (29). A short derivation leads to the choice of quadrant as:

$$\sin\theta_{\mathrm{xx}} = -\left[e\cos\omega - \mathrm{sgn}^*(\cos\omega)\sqrt{1-e^2\sin^2\omega}\right]\sin\omega \tag{32}$$

$$\cos\theta_{\mathrm{xx}} = -e\sin^2\omega - |\cos\omega|\sqrt{1-e^2\sin^2\omega} \tag{33}$$

$$\mathrm{sgn}^*(\cos\omega) = \begin{cases} \mathrm{sgn}(\cos\omega) & \text{if } \cos\omega \neq 0 \\ \pm 1 & \text{if } \cos\omega = 0 \end{cases} \tag{34}$$

The corresponding maximum value of $\dot{i}_{\mathrm{x}}$ is then found to be

$$\dot{i}_{\mathrm{xx}} = \frac{pf}{h\left(\sqrt{1-e^2\sin^2\omega} - e|\cos\omega|\right)} \tag{35}$$

Longitude of the Ascending Node

The analysis for Ω is analogous to the one for inclination, given the similar functional form of the variational equations, (1) and (2), for these elements. The following results are obtained:

$$\beta_{\mathrm{x}} = \mathrm{sgn}[\sin(\theta+\omega)]\frac{\pi}{2} \tag{36}$$

$$\dot{\Omega}_{\mathrm{x}} = \frac{r|\sin(\theta+\omega)|}{h\sin i} f \tag{37}$$

$$\cos(\theta_{\mathrm{x}} + \omega) = -e\cos\omega \tag{38}$$

$$\sin\theta_{\mathrm{xx}} = \left[e\sin\omega - \mathrm{sgn}^*(\sin\omega)\sqrt{1-e^2\cos^2\omega}\right]\cos\omega \tag{39}$$

$$\cos\theta_{\mathrm{xx}} = -e\cos^2\omega - |\sin\omega|\sqrt{1-e^2\cos^2\omega} \tag{40}$$

$$\dot{\Omega}_{\mathrm{xx}} = \frac{pf}{h\sin i\left(\sqrt{1-e^2\cos^2\omega} - e|\sin\omega|\right)} \tag{41}$$

where the sgn*() function is defined in Eq. (34).

Maximum Rates of Decrease of Orbit Elements

In the analysis for the argument of periapis, we noted that at any point on the orbit, the sign of $\dot{\omega}$ for in-plane changes may be reversed by thrusting in the opposite direction. By examining the variational equations (1)–(5), this is immediately seen to be true also in the full three-dimensional case, and also for the other four orbit elements. Thus we may write

$$\dot{æ}_{\mathrm{n}} = -\dot{æ}_{\mathrm{x}} \tag{42}$$

$$\dot{æ}_{\mathrm{nn}} = -\dot{æ}_{\mathrm{xx}} \tag{43}$$

$$\alpha_{æ\mathrm{n}} = \alpha_{æ\mathrm{x}} + \pi \tag{44}$$

$$\sin\beta_{æ\mathrm{n}} = -\sin\beta_{æ\mathrm{x}} \tag{45}$$

$$\tag{46}$$

where $æ$ represents in turn each of the five orbit elements Ω, i, ω, a, and e.

TIME-TO-GO CONCEPT

Four guiding principles are used in the time-to-go concept. The first is one of "effectivity." When thrusting is deemed insufficiently effective, thrust is turned off. For example, if we are to change the semimajor axis, without regard for the other elements, the most effective place to do so is at periapsis [Eq. (11)]. As the spacecraft proceeds on the transfer orbit, thrust is discontinued if the effectivity of thrust drops below some specified cut-off level when compared with the effectivity at the osculating periapsis. Specifically, the effectivity is defined as

$$\eta = \frac{\dot{\text{æ}}_{\text{x}}}{\dot{\text{æ}}_{\text{xx}}} \tag{47}$$

Gefert and Hack[2] also introduced this quantity, but only for the apoapsis radius, calling it an efficiency factor. For changing other orbit elements, similar cut-off effectivities are set for the orbit elements in question. The effectivity at any point on an orbit may be immediately computed based on the analytic expressions for $\dot{\text{æ}}_{\text{x}}$ and $\dot{\text{æ}}_{\text{xx}}$. The effectivity is the first input to the time-to-go control law.

The second principle is one of overshooting. It may be beneficial to change an orbit element beyond its target value in order to make it easier to perform required changes in other orbit elements. An obvious example is that of changing inclination and semimajor axis concurrently. For large enough inclination changes, less propellant is required overall if the orbit is first enlarged, the inclination change performed at this enlarged orbit, and finally the orbit reduced to the desired size. Similar trade-offs occur with some of the other orbit elements. The logic for determining when overshooting should occur is based on the changes needed in the elements and the rates of change achievable for these elements on the osculating orbit. In particular, for each orbit element that must be changed, we estimate a lower bound for the minimum time needed:

$$t_{\delta\text{æ}_{\text{ne}}} = \frac{|\text{æ} - \text{æ}_T|}{\dot{\text{æ}}_{\text{xx}}} \tag{48}$$

Taking a transfer in inclination and semimajor axis for example, if $t_{\delta i_{\text{ne}}} \gg t_{\delta a_{\text{ne}}}$, then most of the thrust is used to change a in the initial portion of the transfer. In the middle portion of the transfer, when $t_{\delta i_{\text{ne}}} \not\gg t_{\delta a_{\text{ne}}}$, most of the thrust is used to change i. The numerical meaning of "$\gg$", "$\not\gg$" and "most" is controlled by parameters provided as input to the control law. The maximum permitted overshoot is also an input parameter to the control law.

The third principle, employed towards the end of the transfer when $t_{\delta\text{æ}_{\text{ne}}}$ is roughly equal for each of the orbit elements, is one of thrusting in such a direction that each of the elements has an equal "time-to-go" to its target value. The fourth principle is one of determining a thrust direction when the previous three principles would call for conflicting thrust directions. In the following numerical examples of this section, the fourth principle need not be invoked, as the thrust directions for changing the two orbit elements are uncoupled.

Numerical Example: Transfer in a and i Using Time-to-Go

For a satellite in orbit around the Earth, an inclination change of almost 90° is sought together with an increase in semimajor axis. The other elements are considered free. The relevant initial orbit elements are listed in Table 1, which includes the free e and ω because their values impact the time-to-go control law. The values of i and e are small, but non-zero, to avoid the the well-known singularities in the variational equations when values of zero are attained. The desired final inclination and semimajor axis values are 90° and 10000km, respectively, as shown in Table 1. Table 2 lists the thrust, specific impulse, and initial spacecraft mass. A rather high thrust-to-weight ratio is used, firstly to ease the computational burden of integrating many revolutions around the

central body, and secondly to simplify the graphical presentation of trajectory data (for example, to permit consecutive revolutions on a trajectory plot to be discernible).

Table 1

INITIAL AND TARGET ORBITS: *ai* TRANSFER

Inclination	0.03°	90°
Semimajor axis	7452.7 km	10000 km
Periapsis altitude	1000	*free*
Eccentricity	0.01	*free*
Argument of periapsis	0°	*free*

Table 2

THRUST, SPECIFIC IMPULSE AND INITIAL SPACECRAFT MASS

Thrust	9.3 N
Specific Impulse	3100 s
Initial spacecraft mass	300 kg

Figures 1 and 2 show the time histories of a and i, respectively, based on a time-to-go control law. The semimajor axis increases rapidly, so that most of the plane change can be accomplished at larger orbits where it is more efficient to change the inclination. The control law input parameters determine the steepness of the initial rise and final fall in a, the height and duration of the plateau in a, the size of the small drops in a on the plateau, the corresponding shallow–steep–shallow increase in i, and the presence of coast arcs, where neither element changes. Slightly bigger increases in inclination are seen near apoapsis, rather than near periapsis, since the eccentricity is non-zero and it is more efficient to change inclination at apoapsis for the case $\omega = 0$. The coast segments are rather small, because of the low a and i effectivity cutoffs of 0.8 and 0.5, respectively — these are low given the small eccentricity. The target values of a and i are met to one part in 10^4, and the final eccentricity and argument or periapsis are 0.12 and 111.1°, respectively. The final spacecraft mass is 200.5kg, and the flight time 4.65 days. The transfer orbit is shown in Fig. 3.

Numerical Example: Transfer in a and e Using Time-to-Go

The time-to-go concept is now applied to a satellite in orbit around the Earth, where an increase is sought in both semimajor axis and eccentricity, as shown in Table 3. The thrust and mass parameters are again the ones in Table 2.

Table 3

INITIAL AND TARGET ORBITS: *ae* TRANSFER

Semimajor axis	7452.7 km	10000 km
Periapsis Altitude	1000 km	2621.9 km
Eccentricity	0.2	0.7

The time histories of a and e are shown in Figs. 4 and 5, respectively. Effectivity cutoffs are set at 0.8 for both orbit elements. As a consequence, most of the thrusting occurs near periapsis. The second principle of the time-to-go concept is not invoked, as there is no obvious advantage to be had by overshooting in one element to facilitate changes in the other. The fourth principle prohibits thrusting at apoapsis, where it is most efficient to change e, because the necessary thrust direction would diminish a, contrary to the desired increase. The third principle blends the optimal $\dot{a}$ and $\dot{e}$ thrust directions so that the estimated time to go for the two elements is equal.

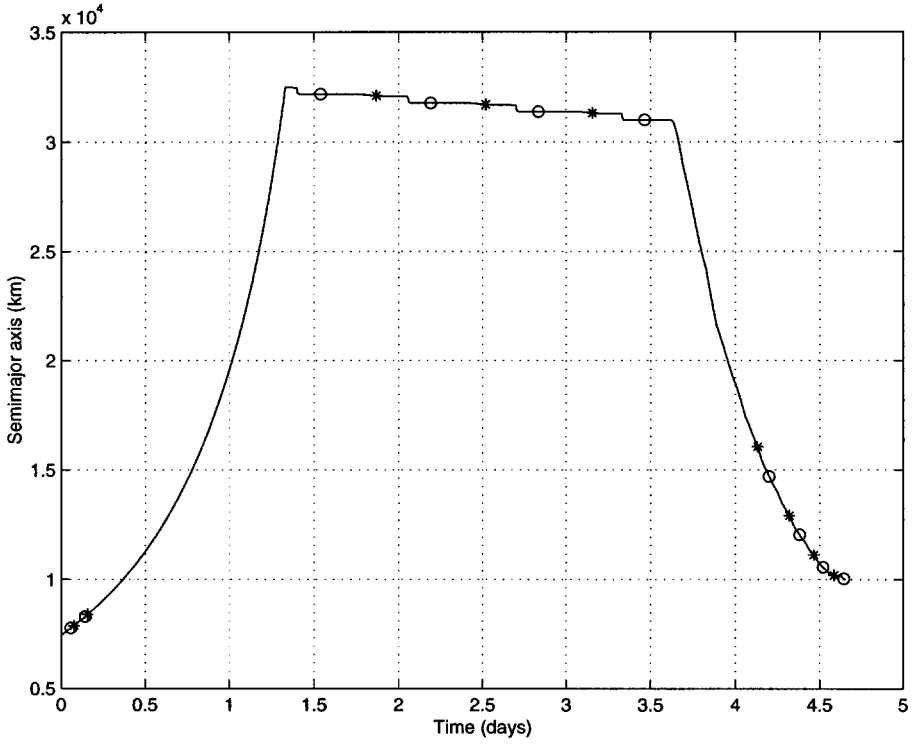

Figure 1 Time-to-go control law for transfer in a and i: Time history of a. Periapsis denoted by $*$, apoapsis by $\circ$.

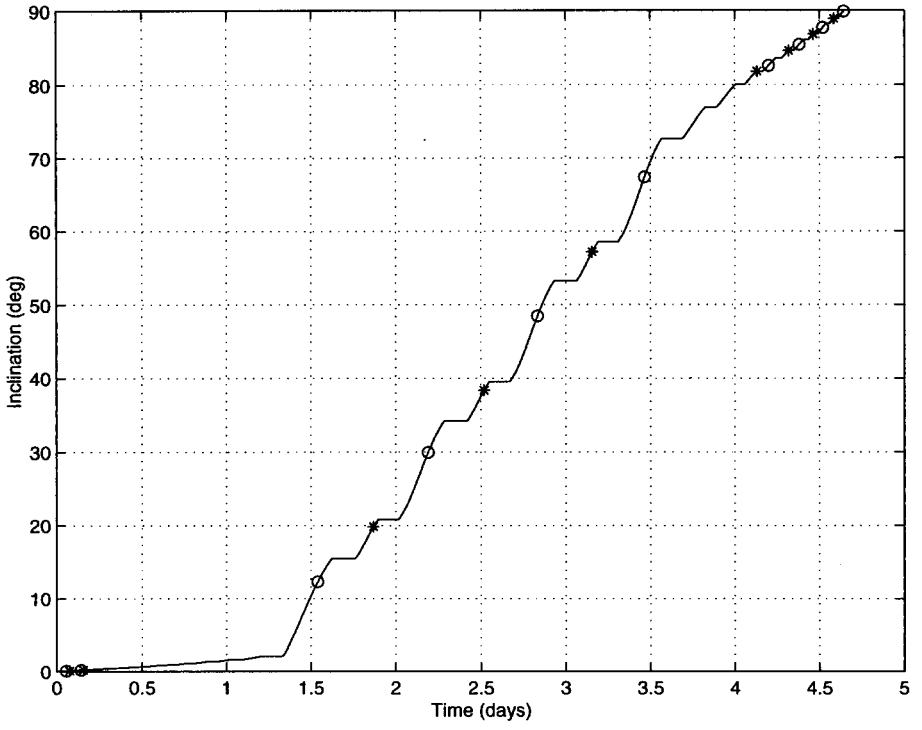

Figure 2 **Time-to-go control law for transfer in a and i: Time history of i. Periapsis denoted by $*$, apoapsis by $\circ$.**

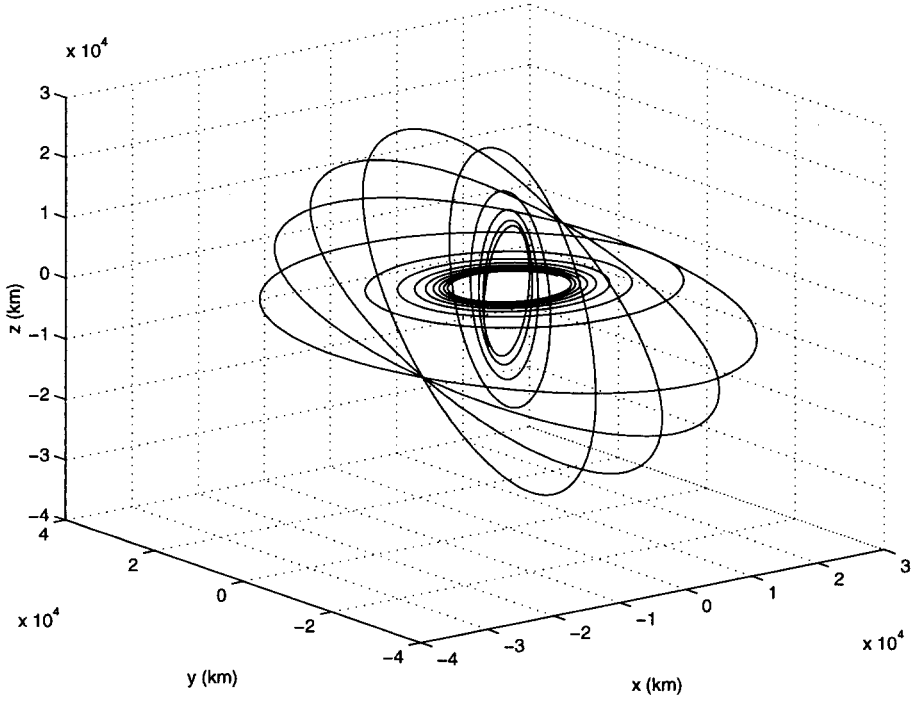

Figure 3 **Time-to-go control law for transfer in a and i: Trajectory plot.**

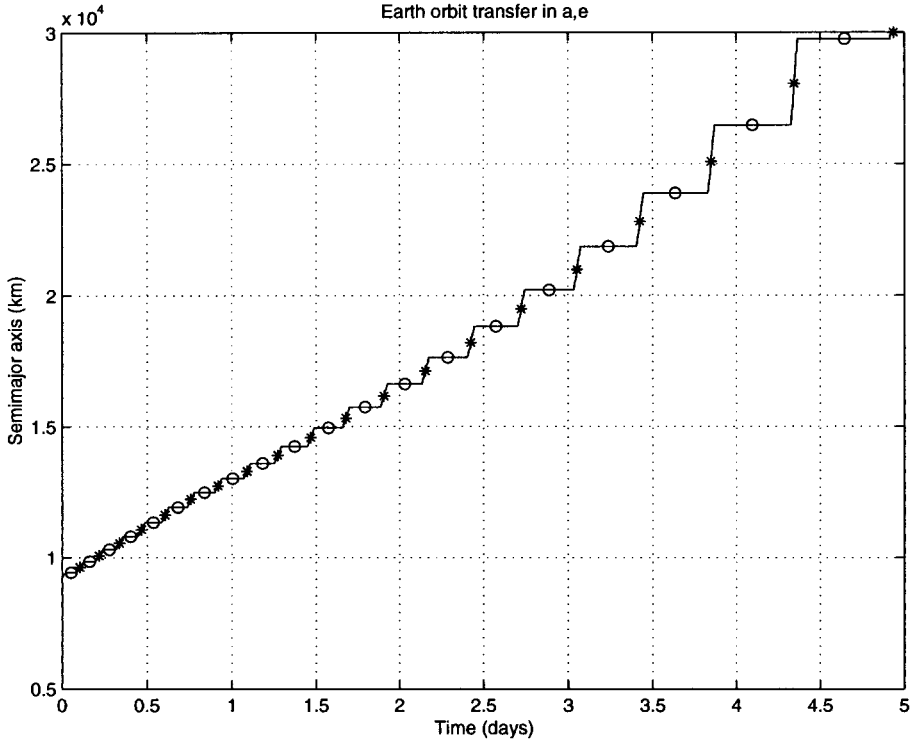

Figure 4 Time-to-go control law for transfer in a and e: Time history of a. Periapsis denoted by $*$, apoapsis by $\circ$.

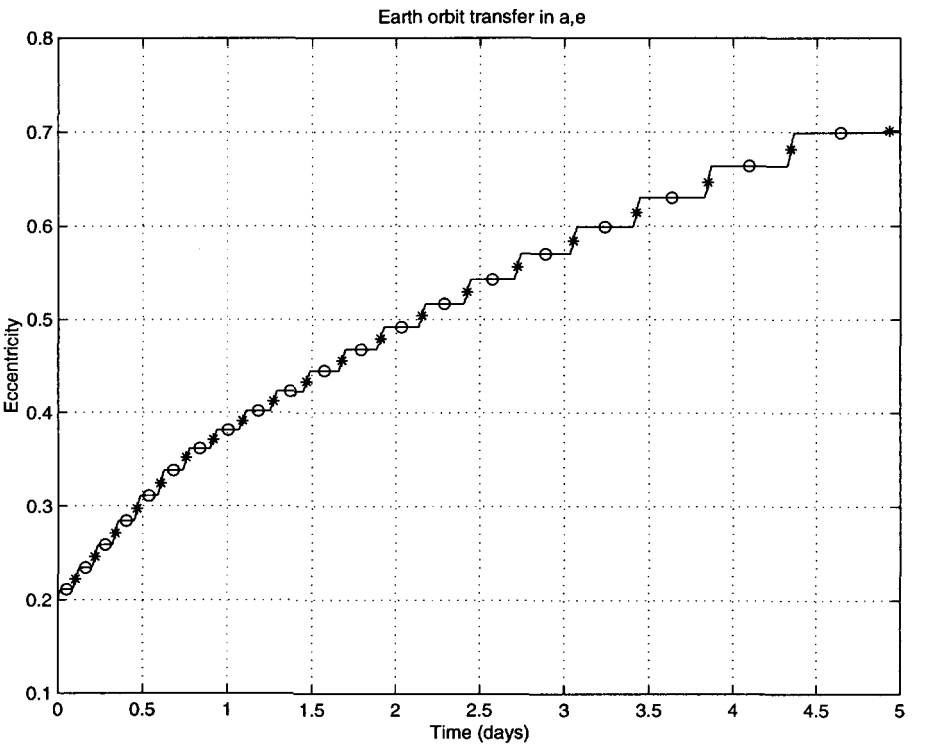

Figure 5 Time-to-go control law for transfer in a and e: Time history of e. Periapsis denoted by $*$, apoapsis by $\circ$.

The target semimajor axis is met within 10km, and the target eccentricity within 0.01. The flight time is 4.923 days, and the final spacecraft mass 278.42kg. These values are shortly compared with values obtained with the proximity-quotient concept and with optimisation.

PROXIMITY-QUOTIENT CONCEPT

The proximity-quotient concept is essentially a systematic encapsulation of the four principles of the time-to-go concept. A proximity quotient is introduced, which judiciously quantifies the proximity of the osculating orbit to the target orbit. Here we take the proximity quotient as

$$Q = \sum_{\text{æ}} W_{\text{æ}} \left(\frac{\text{æ} - \text{æ}_T}{\dot{\text{æ}}_{\text{xx}}} \right)^2 \tag{49}$$

which may be thought of as a "best-case quadratic time-to-go," in that it captures the best possible rate of change for each of the orbit elements over the osculating orbit. The weights, $W_{\text{æ}}$, are always greater than zero, and usually taken as zero or one. Thus, Q is always greater than or equal to zero, and our goal in the orbit transfer is to drive it to zero. We note that Q is a function only of the five orbit elements, and not of true anomaly or the thrust angles. The summation in Eq. (49) is available analytically since analytic expressions have been derived for each or the æ_{xx}. Now, the time rate of change of Q is simply

$$\frac{\mathrm{d}Q}{\mathrm{d}t} = \sum_{\text{æ}} \frac{\partial Q}{\partial \text{æ}} \dot{\text{æ}} \tag{50}$$

where each of the $\dot{\text{æ}}$ are available explicitly from the variational equations (1)–(5). Thus, unlike Q, $\dot{Q}$ depends on the thrust angles. At any point on the transfer, we choose the thrust angles which make $\dot{Q}$ most negative. These angles which minimise $\dot{Q}$ must be found numerically, as an anlytic solution does not appear available. (The numerical search is not excessively time consuming, and so may be easily used in a numerical integration of the variational equations.) With these angles, we ensure that Q is being sent towards zero as quickly as possible at each instant.

The concept of effectivity may be applied to Q as well. If the minimum $\dot{Q}$, $\dot{Q}_{\text{min}}$, is greater than or equal to zero at the current orbit location, then thrust is not applied. Similarly, we can cut off the thrust if $\dot{Q}_{\text{min}}$ is not sufficiently negative, compared, say, with the most negative value that could be attained over the entire osculating orbit. A more practical yardstick for the current $\dot{Q}_{\text{min}}$ might be the minimum value attained by $\dot{Q}_{\text{min}}$ over the preceding revolution. This minimum minimum value of $\dot{Q}$ is easily kept track of in the numerical integration of the variational equations; an initial value must simply be computed for the initial revolution.

There are two complications that have not been excluded analytically, but also which have not been encountered numerically. The first is that we have not proven that it is possible to reduce Q for any osculating and target orbit combinations. The second is that our control law may pull the solution to the wrong local minimum of Q, there being at least two. The first minimum is clearly at the target orbit — this minimum is zero, and has a large region of attraction. The second minimum is at $a = \infty$, where it is always easiest to change all of the orbit elements. Thus, the solution must always be brought into the region of attraction of the minimum at the target orbit, if it every wanders into the region of attraction of another minimum. A contour plot of the Q function, for the case of a transfer in two orbit elements, helps in visualising the local minima. Figure 6 shows such a contour plot for the transfer in semimajor axis and inclination of the preceding section. Superimposed on the contour plot is the path taken by the transfer computed with the time-to-go control law. The contour lines show that there is a saddle in Q near $a = 40000$km and $i = \pi/2$. The minimum in Q due to the target orbit is to the left of the saddle, while the minimum at infinity is to the right of the saddle. In this case the time-to-go control law takes the transfer directly into the region of attraction of the correct local minimum. We now demonstrate the proximity-quotient control law with a transfer in semimajor axis and eccentricity.

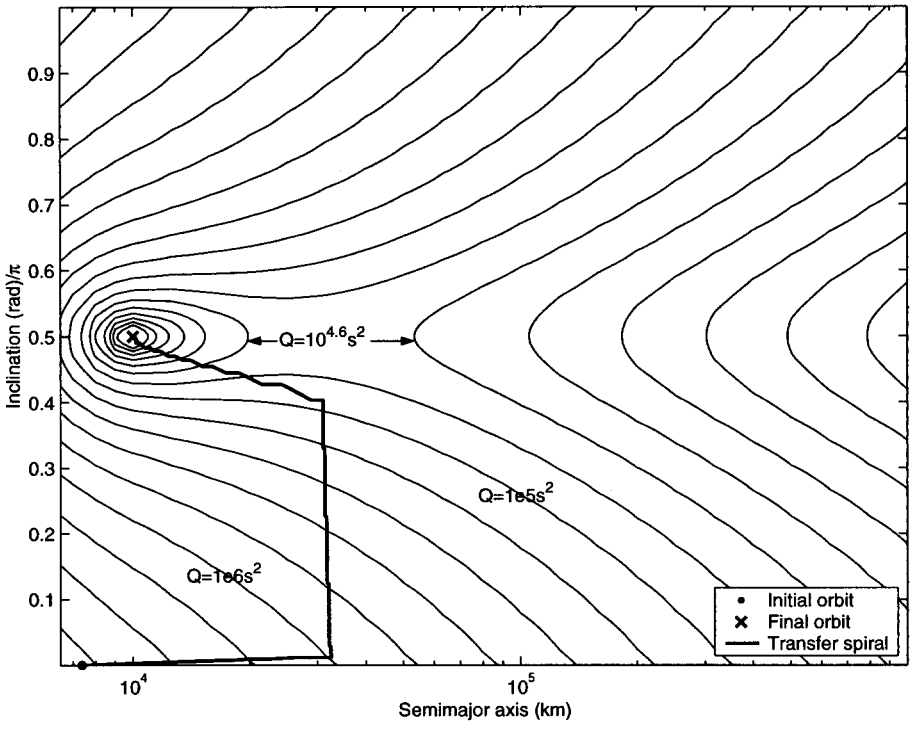

Figure 6 **Contours of the proximity quotient for the *ai* transfer of Tables 1 and 2. The transfer computed with the time-to-go control law, shown in Figs. 1–3, is superimposed on the contour plot.**

Numerical Example: Transfer in a and e Using the Proximity Quotient

We consider here the same transfer in semimajor axis and eccentricity as we did with the time-to-go control law. The weights for semimajor axis and eccentricity, W_a and W_e, are set to one, and the other weights to zero. A sliding effectivity cutoff is used for $\dot{Q}_{\min}$: It remains at 0.6 for $a < 23000$km and then drops gradually to zero as a approaches the target value of 30000km. The effectivity cutoff controls the number of revolutions and time needed for the transfer.

Figures 7 and 8 show the variation in semimajor axis and eccentricity with true anomaly. The transfer itself is plotted in Fig. 9. The transfer takes 19.63 revolutions, 4.50 days, and has a final mass of 280.96kg. Figure 10 shows the a contour plot of the proximity quotient for this transfer, as well as the path taken by the transfer in ai-space.

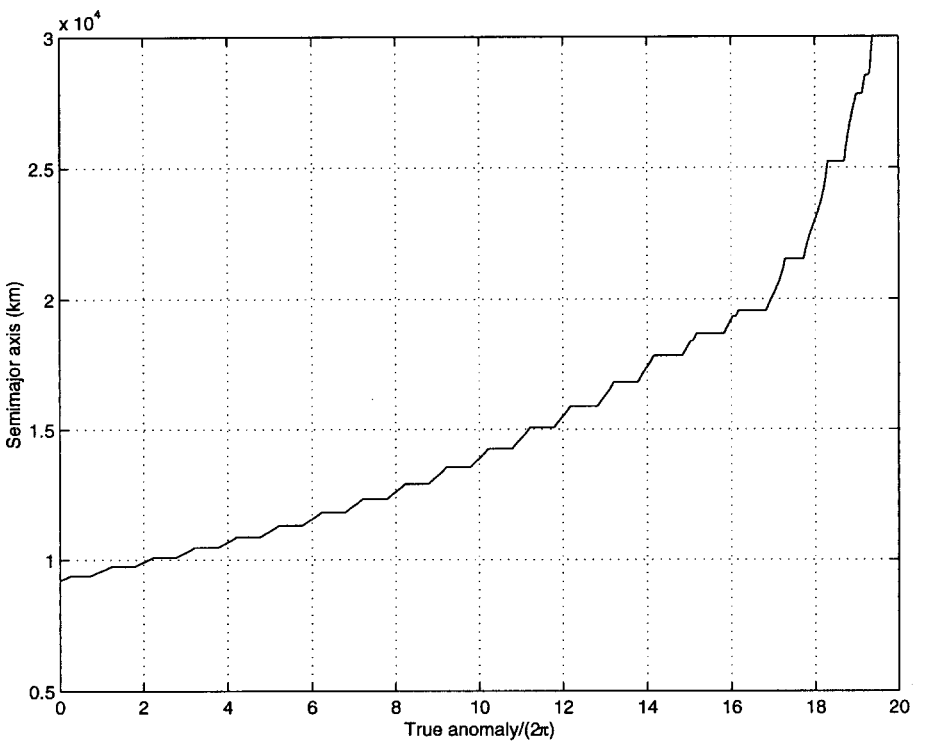

Figure 7 Proximity-quotient control law for transfer in a and e: a as a function of true anomaly.

COMPARISON WITH OPTIMISED TRANSFER

For the purposes of assessing the efficacy of the new control laws, we study here the same transfer in semimajor axis and eccentricity as in the previous two sections. We seek to maximise the final spacecraft mass, and constrain the flight time to be equal to the transfer time of the time-to-go case (4.923 days). The optimisation software used is based on the static/dynamic control (SDC) algorithm.[4–6] SDC best fits into the direct method category, although, unlike other direct methods, the explicit time dependence of the optimisation problem is not removed by parametrisation.

The initial guesses to the optimiser were normally obtained by rather simply applying thrust partly along the velocity vector and partly perpendicular to the line of apsides. Several different propellant-optimal transfers were found, corresponding to different initial guesses. The different

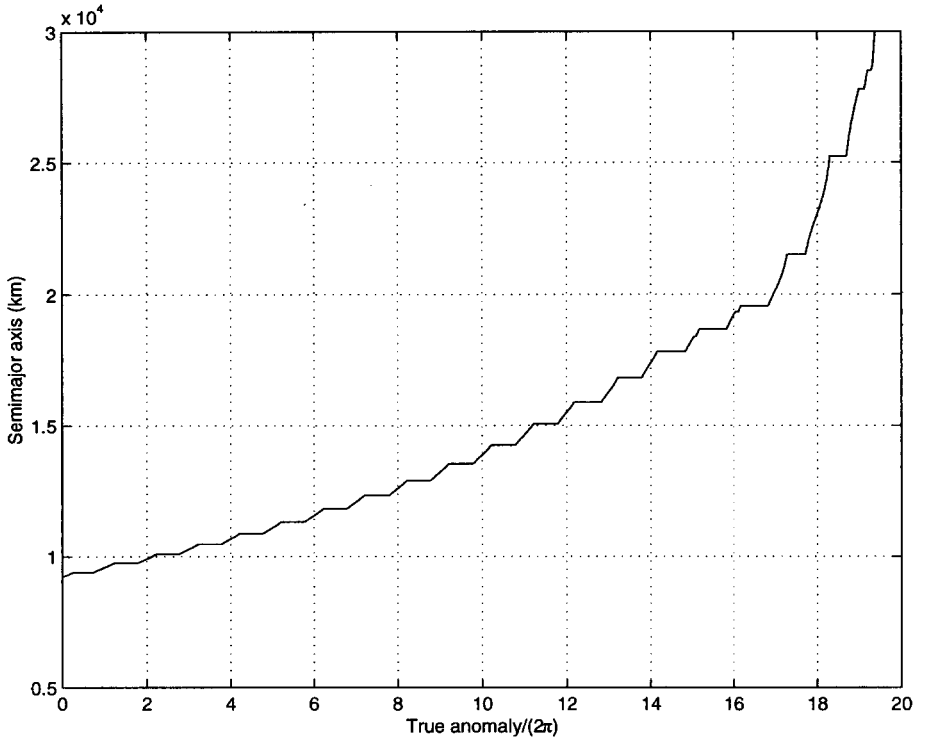

Figure 8 Proximity-quotient control law for transfer in a and e: e as a function of true anomaly.

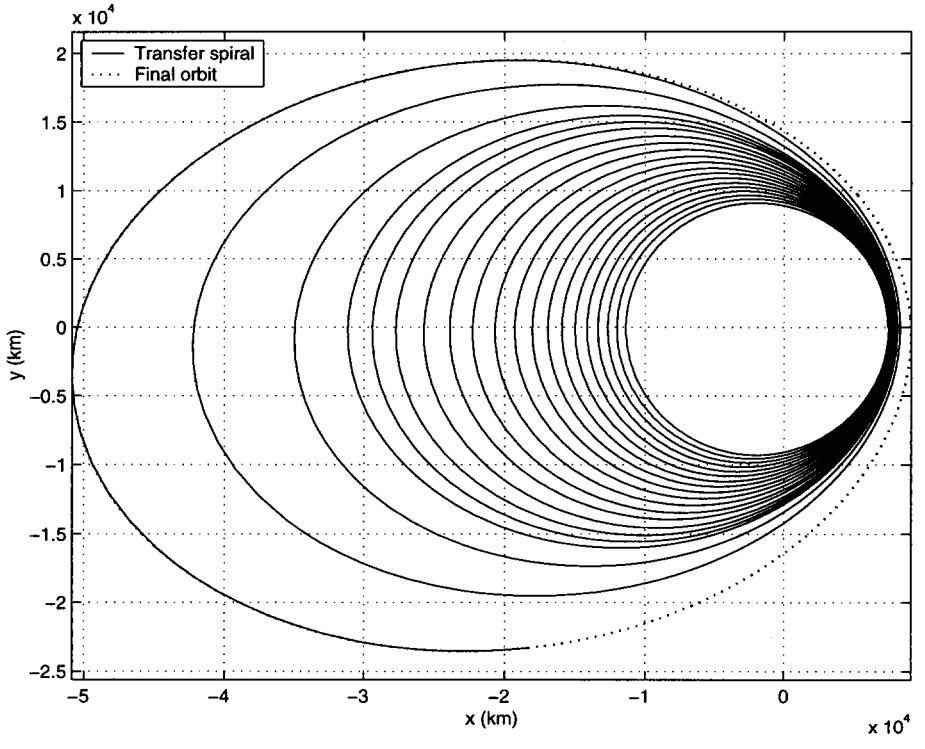

Figure 9 Proximity-quotient control law for transfer in a and e: Trajectory plot.

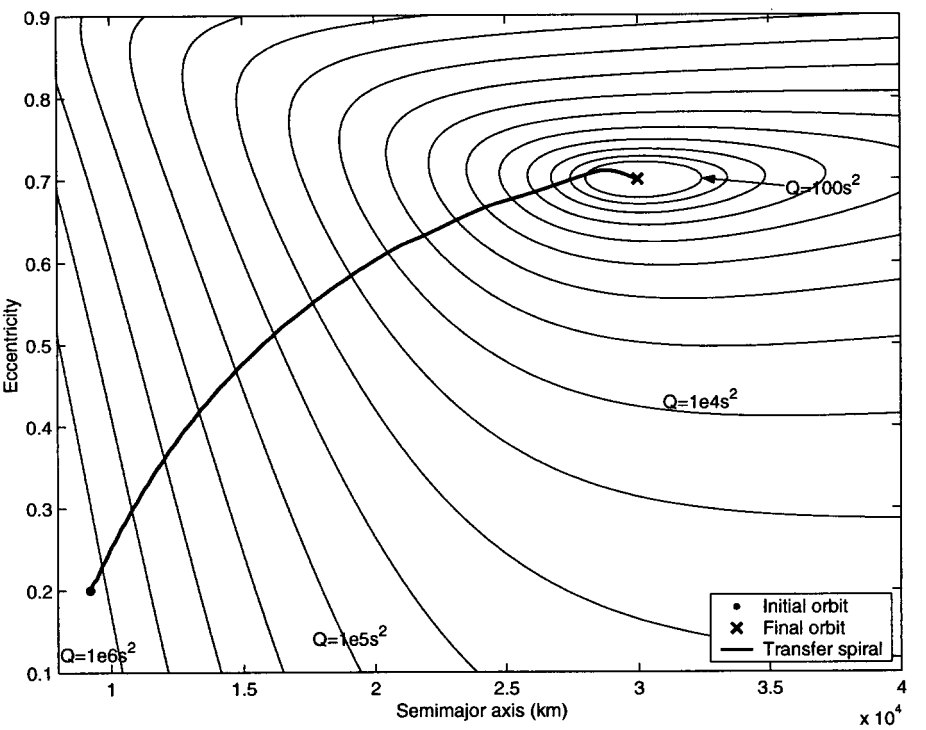

Figure 10 **Contours of the proximity quotient for the *ae* transfer of Tables 2 and 3. The transfer computed with the proximity-quotient control law, shown in Figs. 7–9, is superimposed on the contour plot.**

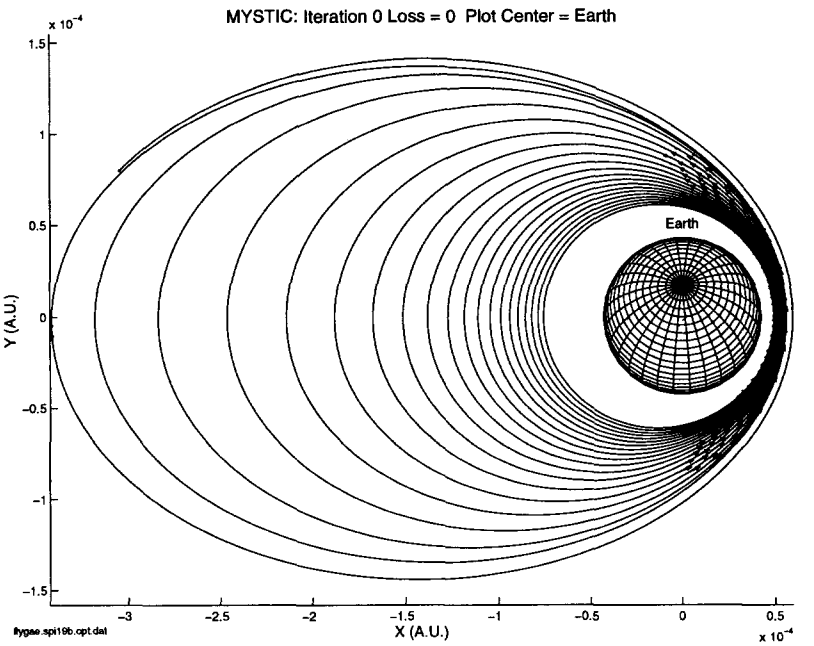

Figure 11 SDC-optimised transfer trajectory for the transfer of Tables 2 and 3.

local optima normally had different numbers of full orbit revolutions, although some local optima had the same number of full revolutions. Figure 11 shows the best local optimum obtained for the case of 20 full revolutions. The arrows represent thrust. We note that the last thrust occurs near the final apoapsis, that is, at 19.5 revolutions. The transfer then continues for almost a full revolution without thrusting. The final orbit period is 0.60 days. Table 4 compares the characteristics of this optimal transfer with the transfers obtained with the time-to-go and proximity-quotient control laws.

Table 4

COMPARISON OF ae TRANSFERS

	Time-to-go law	Proximity-quotient law	SDC-optimised
Initial mass, kg	300	300	300
Final mass, kg	278.42	280.96	281.49
Transfer time, days	4.923	4.50	4.923[a]
Number of revolutions	19.84	19.63	20.45[a]
Last thrust Revolution	19.84	19.63	19.50

[a]Last thrust occurs almost one full revolution (0.6 days) prior thereto.

As seen in Table 4 and in Figs. 9 and 11, the proximity-quotient transfer is quite similar to the optimised SDC transfer. The more heuristic time-to-go control law does not match the SDC solution quite as well. Interestingly, the proximity-quotient transfer, like the optimal SDC transfer, demonstrates a small overshoot in eccentricity.

CONCLUSIONS

Based on Gauss's form of the variational equations, we have derived analytic expressions for the optimal thrust direction and location on the osculating orbit for changing each of the orbit elements except true anomaly. As a consequence, the corresponding rate of change of each orbit element is also known anlytically. We capitalise on these the analytic expressions in two control law concepts: The time-to-go concept and the proximity-quotient concept. The latter concept formalises analytically the heuristics of the former concept, by introducing a function called a proximity quotient, which assesses the proximity of the current orbit to the target orbit. In at least one test case, that of a transfer in semimajor axis and eccentricity, the proximity-quotient approach closely models the optimal transfer. Use of the proximity-quotient approach is expected to be fruitful also for more intricate orbit transfers.

ACKNOWLEDGEMENTS

This research was carried out at the Jet Propulsion Laboratory, California Institute of Technology, under a contract with the National Aeronautics and Space Administration. The author is indebted to Gregory Whiffen for the mentoring in the use of his SDC optimisation software.

NOTATION

a	semimajor axis (m)
e	eccentricity
f	acceleration due to thrust (m/s^2)
h	specific angular orbital momentum (m^2/s)
i	inclination (rad)
p	semilatus rectum (m)
r	radial distance from central body (m)
$t_{\delta æ_{\mathrm{ne}}}$	estimated lower bound for the minimum time needed for a change in $æ$ (s)
v	velocity (m/s)
R	unspecified auxilliary function used in specifying 4-quadrant angles
Q	proximity quotient (s^2)
$W_{æ}$	Weight for orbit element $æ$
$æ$	orbit element (one of a, e, i, ω, Ω)
α	Angle of the projection of the thrust onto the orbit plane with respect to the local horizon, positive outwards (rad)
β	Angle between the thrust and the orbit plane, positive in the direction of the orbital angular momentum (rad)
η	effectivity factor
θ	true anomaly (rad)
μ	gravitational parameter of the two-body system (m^3/s^2)
ϕ	an auxilliary phase angle (rad)
ω	Argument of periapsis (rad)
Ω	Longitude of the ascending node (rad)
$()_{\mathrm{x}}$	maximum over thrust angle, or giving said maximum
$()_{\mathrm{xx}}$	maximum over true anomaly of the maximum over thrust angle, or giving said maximum
$()_{\mathrm{n}}$	minimum over thrust angle, or giving said minimum
$()_{\mathrm{nn}}$	minimum over true anomaly of the minimum over thrust angle, or giving said minimum
$()_h$	component along the orbital angular momentum vector
$()_r$	radially outward component
$()_\theta$	circumferential component
$()_T$	target value
$\dot{()}$	derivative with respect to time

REFERENCES

1. Kluever, C. A., "Simple Guidance Scheme for Low-Thrust Orbit Transfers," *J. Guidance, Control, and Dynamics,* Vol.21, No.6, Nov. 1998, pp.1015–1017.
2. Gefert, L. P. and Hack, K. J., "Low-Thrust Control Law Development for Transfer from Low Earth Orbits to High Energy Elliptical Parking Orbits," AAS/AIAA Astrodynamics Specialist Conference, AAS Paper 99-410, Girdwood, Alaska, Aug. 1999.
3. Battin, R. H., *An Introduction to the Mathematics and Methods of Astrodynamics,* 1st ed. 4th printing, AIAA, New York, 1987, pp.488–489.
4. Whiffen, G. J. and Sims, J. A., "Application of a Novel Optimal Control Algorithm to Low-Thrust Trajectory Optimization," AAS/AIAA Space Flight Mechanics Meeting, AAS Paper 01-209, Santa Barbara, California, Feb. 11-15, 2001.
5. Whiffen, G. J. and Sims, J. A., "Application of the SDC Optimal Control Algorithm to Low-Thrust Escape and Capture Trajectory Optimization," AAS/AIAA Space Flight Mechanics Meeting, AAS Paper 02-208, San Antonio, Texas, Jan. 27-30, 2002.
6. Whiffen, G. J. and Sims, J. A., "Application of the SDC Optimal Control Algorithm to Low-Thrust Escape and Capture Including Fourth-Body Effects," Proceedings of the 2nd International Symposium on Low Thrust Trajectories, Toulouse, France, June 18-20, 2002.